Computational and Structural Biotechnology Journal 28 (2025) 199–210

Contents lists available at ScienceDirect

Computational and Structural Biotechnology Journal

journal homepage: www.elsevier.com/locate/csbj

Research Article

Inertial sensor-based gait classification for frailty status in older adults: A cross-sectional study

Wei-Chih Lien [a,b,1], Wen-Fong Wang [c,*,1], Chien-Hsiang Chang [d], Bo Liu [d], Yi-Ching Yang [e,f], Tai-Hua Yang [g,h], Ta-Shen Kuan [a,b], Wei-Ming Wang [i], Wei Huang [c], Danyal Shahmirzadi [c], Yang-Cheng Lin [d,**]

[a] Department of Physical Medicine and Rehabilitation, National Cheng Kung University Hospital, College of Medicine, National Cheng Kung University, Tainan, Taiwan
[b] Department of Physical Medicine and Rehabilitation, College of Medicine, National Cheng Kung University, Tainan, Taiwan
[c] Department of Computer Science and Information Engineering, National Yunlin University of Science and Technology, Douliu, Yunlin, Taiwan
[d] Department of Industrial Design, National Cheng Kung University, Tainan, Taiwan
[e] Department of Family Medicine, National Cheng Kung University Hospital, College of Medicine, National Cheng Kung University, Tainan, Taiwan
[f] Department of Family Medicine, College of Medicine, National Cheng Kung University, Tainan, Taiwan
[g] Department of Orthopedics, National Cheng Kung University Hospital, College of Medicine, National Cheng Kung University, Tainan, Taiwan
[h] Department of Biomedical Engineering, National Cheng Kung University, Tainan, Taiwan
[i] Department of Statistics and Information Science, Fu Jen Catholic University, New Taipei City, Taiwan

ARTICLE INFO

Keywords:
Frailty diagnosis
Gait assessment
Machine learning

ABSTRACT

Frailty in older adults is caused by functional declines that result in unstable gait. This study analyzed gait in 24 frail and 22 non-frail older adults using acceleration and angular velocity signals from a wireless tri-axial inertial measurement unit (IMU). After noise was removed through Savitzky-Golay and Butterworth filters, gait features correlated with frailty were proposed and evaluated through normality tests and statistical analysis. To evaluate the frailty of older adults based on significant gait features derived from statistical analysis, the primary accuracy achieved is roughly around 84–89 % in k-nearest neighbor, support vector machine, and random forest models. To provide clinicians with a good tool for monitoring frailty and support preventive healthcare and aging-in-place strategies, we propose a gait-based detection system with an optimal feature extraction scheme that can exhaustively enumerate and evaluate potential parameters for optimal performance. This system significantly improved classification metrics (nearly all >95 %) with lower sensitivity and specificity and achieved 96 % accuracy with a portable, low-cost system that uses only one minute of walking data. These findings demonstrate that IMU-based gait analysis improves objectivity and accuracy in frailty classification. The optimal feature extraction scheme further refines performance, offering a scalable and time-efficient solution for community-based frailty detection. This approach highlights the potential of wearable sensors in improving geriatric health assessments.

1. Introduction

Frailty is an age-related syndrome strongly associated with impaired activities of daily living (ADLs), reduced mobility, falls, hospitalization, and mortality [1,2]. One prior meta-analysis found that the occurrence of frailty among older adults (>60 years) living in the community is

Abbreviations: ADLs, activities of daily living; ICTs, information and communication technologies; IMU, inertial measurement unit; CHS, Cardiovascular Health Study; BLE, Bluetooth Low Energy; MCU, Microcontroller Unit; RSS, root sum square; SG, Savitzky–Golay; SD, standard deviation; IQR, interquartile range; GCI, single-stride gait cycle interval; GCP, 5-stride gait cycle period; KNN, k-nearest neighbor; SVM, support vector machine; RF, random forest; SA, statistical analysis; ES, element set; GPU, Graphics Processing Unit; TP, true positive; FP, false positive; FN, false negative; TN, true negative.

* Correspondence to: Department of Computer Science and Information Engineering, National Yunlin University of Science and Technology, No.123, University Road, Douliu, Yunlin 640, Taiwan.
** Correspondence to: Department of Industrial Design, National Cheng Kung University, No.1, University Road, Tainan 701, Taiwan.
E-mail addresses: wwf@yuntech.edu.tw (W.-F. Wang), lyc0914@mail.ncku.edu.tw (Y.-C. Lin).
[1] Contributed to this article equally.

https://doi.org/10.1016/j.csbj.2025.05.011
Received 17 December 2024; Received in revised form 11 May 2025; Accepted 11 May 2025
Available online 28 May 2025
2001-0370/© 2025 The Authors. Published by Elsevier B.V. on behalf of Research Network of Computational and Structural Biotechnology. This is an open access article under the CC BY-NC-ND license (http://creativecommons.org/licenses/by-nc-nd/4.0/).

affected by the diagnostic criteria and national income level; a global meta-analysis reported a pooled incidence of 62.7 cases of frailty per 1000 person-years among community-dwelling older adults worldwide [1]. Further, another recent review indicated a pooled frailty prevalence rate of 10.7 % among older adults living in the community [3], while another current meta-analysis found that the pooled prevalence of frailty among community-dwelling adults aged 60 years and older was 20.5 % in Asia [4]. Frailty is a common health problem in older people and is associated with a gradual decline in skeletal muscle mass and strength, resulting in gait patterns that are typically slower, with reduced step length and increased variability, compared with robust individuals. Therefore, understanding the gait patterns of older adults with frailty and developing effective assessment methods is urgently needed and worthy of research to facilitate the development of barrier-free detection of frailty.

Gait analysis is used to explore a person's manner of walking and provide information about walking or other body movements. In research on gait analysis, the deteriorating gait of older adults has become a novel and noteworthy topic due to the aging population in many developed countries. In the literature, Hommen et al. [5] reported differences in step length, stance time, and swing time between healthy and frail older adults. Moreover, Martinikorena et al. [6] pointed out that gait variability is a reliable measure of frailty, while Valdés-Aragonés et al. [7] proposed that monitoring gait could represent an effective method for improving health outcomes regarding frailty and functional status in older adults. However, most of the gait analysis systems currently available share the disadvantage of being expensive, time-consuming, and complex.

In recent years, information and communication technologies (ICTs) have increasingly been proposed as interventions to support older adults affected by various clinical conditions who have difficulty accessing healthcare services [8]. The idea of utilizing telemedicine systems to support remote detection and diagnosis of frailty through gait testing, with the help of ICT, seems promising. Overall, available results indicate that ICTs can positively impact the wellness of older adults by improving their access to healthcare services, enhancing their quality of life, empowering them to maintain a healthy lifestyle, and supporting their social participation [9]. Although there is significant interest in using ICTs for the clinical management of older adults, few studies have specifically focused on investigating how ICTs can be used to identify frailty in older people, primarily via artificial intelligence in the community-based health management of older adults [10]. Notable exceptions include Minici et al. [11], who proposed an automated frailty assessment using a wrist-worn device with 91 % sensitivity and 82 % specificity, and Camerlingo et al. [12], who explored the feasibility of monitoring gait and physical activity in free-living environments.

An inertial measurement unit (IMU) measures the motion of an object. It consists of sensors such as accelerometers, gyroscopes, and magnetometers; this device is small and lightweight. These sensors can be easily installed on different parts of the human body, including the waist, tibia, and ankle, which means that IMUs are widely used in posture assessment and gait analysis. Several studies have introduced the application of inertial sensors in gait analysis. For example, Seel et al. [13] utilized accelerometers and gyroscopes to extract acceleration and angular velocity data to calculate joint angles in the human body. The trunk inclination angle and sacral extension mobility, measured using tri-axial accelerometers, have a fair discriminative power to distinguish older people with a greater risk of falling from those without, and could be considered as therapeutic targets [14]. Suri et al. also used accelerometer signals and correlation coefficients to measure gait stability and identify gait patterns during ambulation on an uneven surface in older adults [15].

Gait analysis can help to clarify the fundamental mechanisms underlying both motor and cognitive decline. Recent advances in technology may enhance the application of gait assessments in various clinical settings, particularly among frail older adults [16]. Research has shown that combining different gait parameters can improve the prediction of falls in sarcopenic older adults with end-stage kidney disease [17]. During this assessment, medical experts use the clinical symptoms of the patient, the medical history, and the results of physical examinations to evaluate gait. However, existing gait assessment methods for frailty are subjective, time-consuming, and difficult for older adults to access in community-based health management using artificial intelligence. Therefore, the present study aimed to improve frailty diagnosis and gait assessment in older adults. We utilized inertial sensors installed within IMUs to collect gait signals and employed supervised machine-learning classification schemes for their analysis. To increase the performance of the classification schemes, we adopted autocorrelation and cross-correlation techniques to create new data domains for frailty evaluation and classification. To our knowledge, this is the first study to use instrumental gait analysis for frailty diagnosis.

2. Material and methods

2.1. Equipment and gait experiment

Participants in the present study were recruited from our institution's community health centers, which supported this study. All participants provided written informed consent. We recruited 55 participants all older than 60 years from February 4, 2021, to January 31, 2023, who: (1) regularly participated in health-promoting activities at their community health center; (2) were able to perform simple movements as required; (3) demonstrated average cognitive ability, as indicated by a total score of eight or more on the Chinese version of the Short Portable Mental State Questionnaire (SPMSQ) [18]; and (4) could understand and follow the instructions of the researchers. Those who met only 1–2 criteria for the frailty phenotype of the Cardiovascular Health Study (CHS) were excluded (n = 9). While those who met the criteria for the frailty phenotype of the CHS, with three or more of the five components (decreased grip strength, unintentional weight loss, reported exhaustion, low physical activity, and decreased gait speed) evaluated according to a predefined protocol [19] were classified into the frail group, and those who did not meet any of the five CHS frailty criteria were classified into the non-frail control group. The non-frail control group was matched by age range and assessed using the same evaluation protocol as the frail group. A schematic presentation of the experimental workflow is shown in Fig. 1(a).

The gait measurement instrument used in this study was a wireless IMU module developed in our laboratory. The sensor module consisted of a Bluetooth Low Energy (BLE)-enabled system chip (Microcontroller Unit [MCU] Model: MDBT40, Raytac Corporation), an IMU (Model: BNO055, Bosch Sensortec), and a power supply unit with a lithium battery.

During the acquisition of the gait signal, the sampling rate of the IMU module was set to 100 Hz. Following capture of the raw gait signal, these data were transmitted via Bluetooth connection to mobile phones or tablets and then uploaded to a computer workstation through a cloud network for further processing and intelligent classification of frailty (Fig. 1(b)). The raw gait signals were stored in JSON file format, while subsequent processing and analysis were performed using signal processing programs coded in the Python 3 programming language with pandas, Numpy, and scikit-learn libraries.

To perform gait tests, a wireless IMU was fixed to each of the participants' legs (approximately 2.5 cm above their feet) using Velcro straps. Subsequently, the power supply for the sensors and the Bluetooth function of a tablet computer were turned on to ensure that the tablet could send control commands to the sensors and receive the detected gait signals from the sensors.

The test was carried out in an obstacle-free space with a straight-line distance of at least 10 m as used in the geriatric clinic for walking tests [17]. A triangular cone marker was placed 10 m from the starting point, while the participants were instructed to walk back and forth between

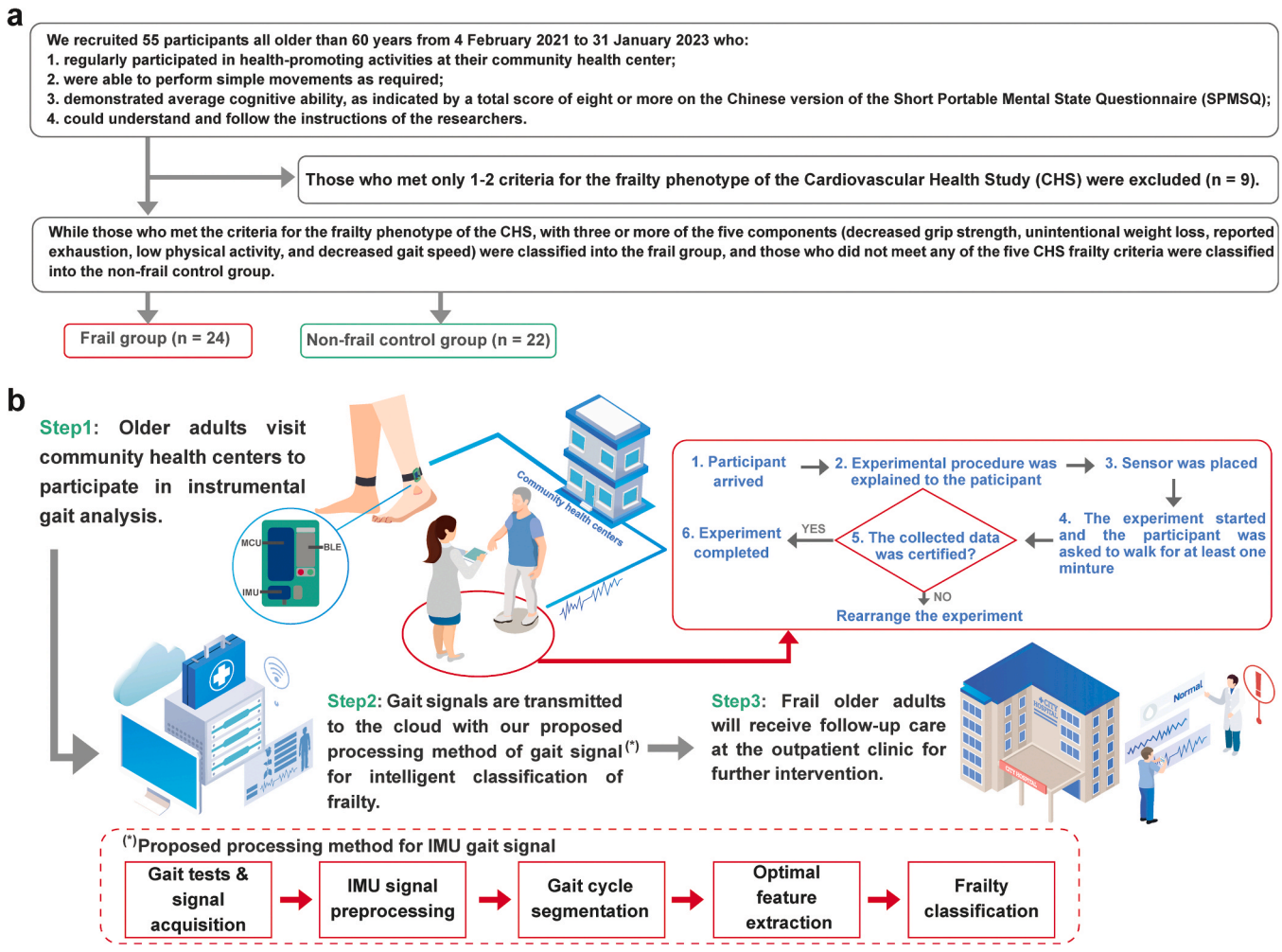

Fig. 1. Illustration of (a) the study case enrollment process and (b) the gait sensor module, instrumental gait analysis workflow in the community health centers, and the data transmission and frail older adults' care service flowchart (https://ehealth.web2.ncku.edu.tw/p/412–1211-26813.php?Lang=zh-tw). MCU: Microcontroller Unit; IMU: inertial measurement unit; BLE: Bluetooth Low Energy.

the starting point and the location of the cone marker for at least 1 minute. During this period, the researchers walked approximately 1 m behind them to ensure their safety.

Before starting the test, participants were guided to their designated positions to ensure proper arrangement. The researchers initiated a countdown sequence before pressing the 'start' button displayed on the screen of a portable tablet after the countdown ends to activate the IMUs. To ensure that the walk time exceeded 1 minute, the researchers conducted another countdown before the test ended.

2.2. Signal preprocessing

To eliminate the calibration issue caused by potential wearing-orientation errors of the IMU during each wear, and considering the features of three-dimensional acceleration, the root sum square (RSS) method was adopted to remove the directional nature of the tri-axial signal and to preserve the original magnitude of acceleration. The calculation formula used for the RSS method is presented below (Eq. (1)):

$$RSS = \sqrt{x^2 + y^2 + z^2} \quad (1)$$

where the variables x, y, and z represent the values of the acceleration component along the x-, y-, and z-axes of the acceleration signal, respectively.

In the present study, different filters and filter parameter settings were applied to process the tri-axial acceleration and angular velocity signals collected by the IMU, owing to variations in features and frequencies. To ensure the accuracy of subsequent signal processing and analysis, the filtered acceleration and angular velocity signals excluded those signals obtained during the experiment at the beginning, end, turns, *etc.* without a stable complete gait cycle (including gait signals that occur before and after turning). Depending on each participant's walking speed, within the 7-second timeframe, approximately 5–8 complete gait cycles of signals were recorded.

During walking tests, vibrations generated by contact between participants' feet and the ground may interfere with the reception of angular velocity signals by the gyroscope, resulting in irregular high-frequency noise in the signal. To address this issue, Savitzky–Golay (SG) filters were applied to eliminate high-frequency noise [20]. The SG filter is a digital signal processing filter that effectively smooths gait signals while preserving gain trends and important features, thus removing high-frequency noise. The parameters used for SG filtering are 1) the window size, which is the number of signal samples that form the window around the sample being filtered, and 2) the filter polynomial order, which is the degree of the least-squares fitted polynomials used in the filter. To smoothen the high-frequency noise of normal gait movements while preserving important gait features, we used a parameter setting with a larger window size and lower polynomial order to more effectively eliminate the high-frequency noise.

Thus, the window size of the SG filter was set to 21, and the order was

set to 3. Fig. 2 presents the changes before and after signal filtering on the z-axis of the gyroscope. After the system was subjected to low-pass filtering, the gyroscope signal exhibited a smoothing trend, while high-frequency noise was eliminated.

To manage possible high-frequency noise in the acceleration signal, a Butterworth low-pass filter was utilized [21]. This filter has a maximally flat magnitude response in its passband and can achieve high stopband attenuation while maintaining frequency response flatness. However, the phase response is non-linear in its passband, especially in high-order Butterworth filters, where the signal phase distortion is more obvious. Based on our previous experiments with the Fourier transformation of gait signals, we found that the major signal band of gait signals from participants is lower than 15 Hz. Therefore, a cutoff frequency of 15 Hz and a filter order of 4 were used for the Butterworth filters in the signal preprocessing. The filtered signal waveform on the x-axis of the accelerometer after processing is shown in Fig. 3.

2.3. Gait cycle segmentation

In this study, we found that the angular velocity signal (Fig. 4(a)) demonstrated superior clarity and consistency compared with the acceleration signals of older adults, making it more reliable for segmenting the gait cycle. Therefore, the peak values in Fig. 4(a) were selected as temporal markers to partition the gait acceleration data obtained during the walking tests.

Peaks in the SG-filtered gyroscopic z-axis angular velocity signal were detected using the find_peaks function from Python's SciPy library. Fig. 4(a) illustrates the angular velocity signal for left and right footsteps, with the identified peaks indicating each boundary of the gait cycle. These segmentation points were then assigned to the corresponding RSS acceleration signals from the IMUs (Fig. 4(b)), allowing precise gait cycle segmentation of the acceleration data.

In addition to the methods previously discussed, other visible gait signal features can also be used to segment the swing phase, stance phase, and gait cycle, as illustrated in Fig. 5. For example, the dashed lines in Fig. 5 divide the gyroscope's z-axis signal curve into distinct gait cycles. Each gait cycle consists of two segments: a strong convex curve, indicating rapid angular velocity changes, and a weakly convex curve, reflecting milder variations. Based on this pattern, the onset point (marked as α) can be identified as the beginning of a swing phase within the gait cycle.

In contrast, the solid lines in Fig. 5 divide the accelerometer's x-axis signal curve into gait cycles. Here, the starting point of each gait cycle corresponds to the deepest valley in the acceleration signal (marked as β in Fig. 5), which indicates an abrupt change caused by initial contact. Thus, β can serve as the starting point for a stance phase.

Taken together, α and β mark the time of two key gait events, toe-off and initial contact, respectively, within the signal curves. Beyond gait cycle segmentation, these points can also delineate swing and stance phases within a single cycle.

2.4. Exploring gait features through autocorrelation and cross-correlation

To calculate the autocorrelation/cross-correlation coefficient between the gait information of the two lower extremities [22,23], we assumed that Q is a collection of RSS acceleration signals (see Fig. 4(b)). This collection contained complete RSS acceleration signals from a gait test and was considered the original dataset to calculate the correlation coefficient. Additionally, we assumed that P represents a pattern dataset used to compare similarities between two signals. In this study, P was set as a signal collection consisting of only one gait cycle, and the peak values of the gyroscopic z-axis angular velocity signals were used (Fig. 4 (a)) as segmentation points for the neighboring gait cycles. Each segment between the two peaks was treated as a complete gait cycle signal and used as the pattern dataset, as presented in Fig. 4(b).

Following segmentation, assuming that the original dataset Q contains n data points (with each data point corresponding to 0.01 s) and the length of the pattern dataset P is m data points, the two correlation calculations are performed using the formula below:

$$CCr(t) = \frac{\sum_{i=1}^{N} (p_i - \overline{p})(q_{i+t} - \overline{q}_t)}{\sqrt{\sum_{i=1}^{N} (p_i - \overline{p})^2 \sum_{i=1}^{N} (q_{i+t} - \overline{q}_t)^2}} \quad (2)$$

Among them, t indicates the integer-based index variable, ranging from 1 to (n-m+1); $\overline{p}$ indicates the average value of set P, and $\overline{q}_t$ indicates the average value of a subset of Q (e.g., ($q_{(t+1)}$, …, $q_{(t+n)}$)). For each calculated value of $CCr(t)$, its range is between −1 and 1.

In the gait signals, we extracted signals of the same duration from each gait data set and ensured that this duration included at least five complete gait cycles for each participant. We further calculated the autocorrelation coefficients of the gait acceleration signals of the left (or right) foot (represented by LL and RR, respectively), as well as the cross-correlation coefficients between the left and right feet (or vice versa) (represented by LR or RL) [24]. Consequently, we generated four different correlation sequences: LL, RR, LR, and RL. Each autocorrelation/cross-correlation sequence was obtained using the correlation operation of Eq. (2) on the acceleration signal P of different gait cycles (Fig. 6(a)), after which the average sequence (Fig. 6(b)) was generated as the correlation sequence LL, RR, LR, or RL. The LL and RR sequences were used to reveal the gait stability of walking with the cyclic gait events of one lower limb, and for the LR and RL sequences, the gait symmetry of walking through cyclic gait events of both lower limbs [17].

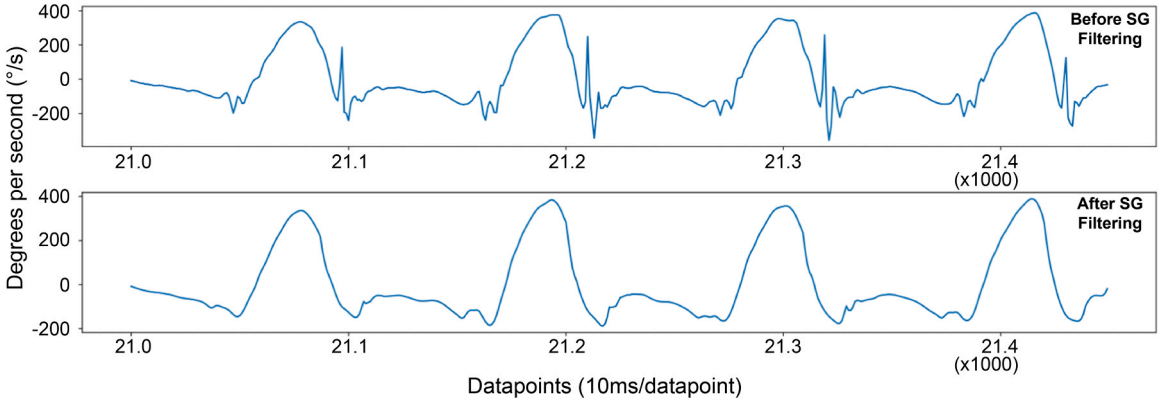

Fig. 2. The angular velocity signal on the z-axis of the gyroscope before and after filtering using a Savitzky–Golay filter.

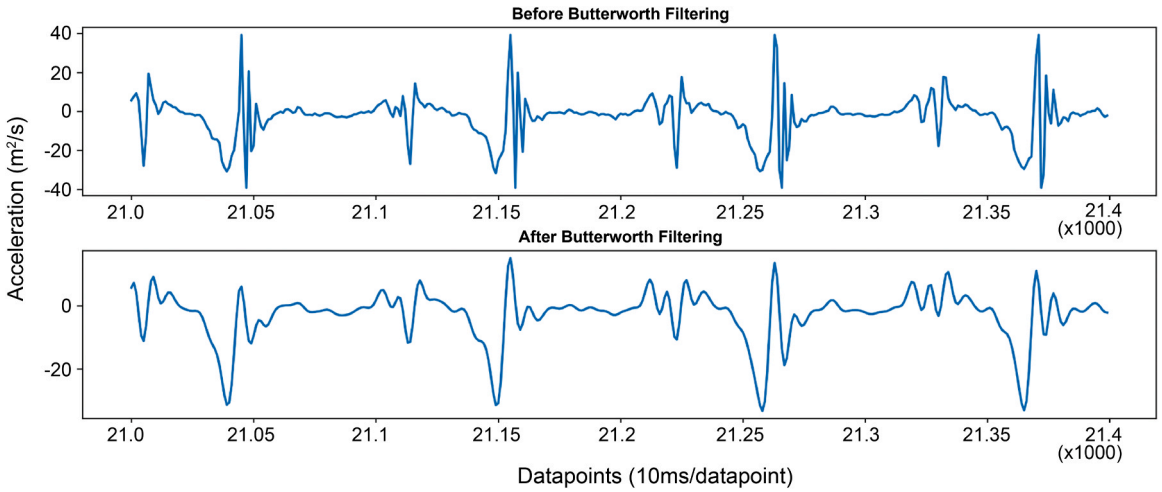

Fig. 3. The acceleration signal on the x-axis of the accelerometer before and after filtering using a Butterworth low-pass filter.

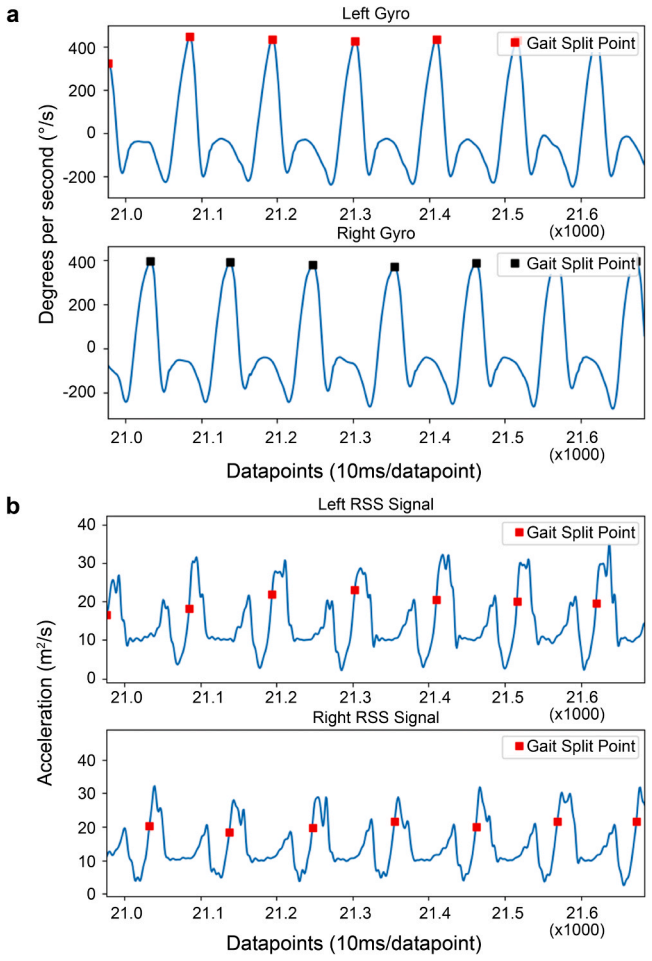

Fig. 4. Continuous gait cycle segmentation: (a) gyroscopic z-axis angular velocity signals of the left and right footstep gait and their corresponding peak points; (b) segmenting the gait cycle of the root sum square (RSS) acceleration signals of the left and right footstep gait using the continuous peak points of the gyroscopic z-axis angular velocity signal.

2.5. Gait feature design

To explore the differences in gait between frail and non-frail participants, we established three types of gait features: parameters from autocorrelation/cross-correlation sequences of gait signals (type 1), gait signal features (type 2), and cumulative correlation parameters (type 3). These features were used to compare the state of frailty according to gait in walking.

The mean (μ) and standard deviation (ρ) of the sets LL, RR, LR, and RL were included as the type 1 gait parameters. Additionally, we chose the parameter variation (V), which calculates the variability among the data elements within each set, as another statistical parameter. This parameter was calculated using the following formula:

$$V = \frac{\max(P\_set) - \min(P\_set)}{mean(P\_set)} \tag{3}$$

where P_set represents one of LL, RR, LR, and RL. *max*(P_set), *min*(P_set), and *mean*(P_set) represent the maximum, minimum, and average values of P_set, respectively.

For the type 2 gait parameters, the cadence, single-stride gait cycle interval (GCI), 5-stride gait cycle period (GCP), stance phase of the gait cycle (%), and swing phase of the gait cycle (%) within a stride cycle were selected as gait feature parameters for the two groups of participants. The cadence, GCI, and GCP were calculated using Eqs. (4), (5), and (6), respectively:

$$Cadence = \frac{number\_of\_qait}{used\_time} * 60 \tag{4}$$

$$GCI(i) = GyroPeaks_i - GyroPeaks_{i-1}, \quad i = 1, \quad 2, \ldots, N \tag{5}$$

$$GCP(i) = GyroPeaks_i - GyroPeaks_{i-5}, \quad i = 5, \quad 6, \ldots, N \tag{6}$$

When calculating the Cadence, the 'number_of_gait' refers to the number of detected gait cycles, while the 'used_time' refers to the time consumed to complete the movement by the detected gait cycles. When calculating the GCI(i), the time for $GyroPeaks_0$ was set to 0, and the time for $GyroPeaks_i$ was set as the time of the ith peak value of the angular velocity in the z-axis of the gyroscope in the IMU.

To compute gait features such as the swing phase ratio (%) and the stance phase ratio (%) within a gait cycle, we used the time of α and β from the sensor signals (Fig. 5). Specifically, for each left and right footstep, α marks the toe-off event on the z-axis of the gyroscope (angular velocity curve), while β corresponds to the initial-contact event on the x-axis of the accelerometer (acceleration curve).

Regarding the cumulative correlation parameters derived from the autocorrelation/cross-correlation sequences of the type 3 gait signals, the correlation sequence curves were divided into two signal curves, Area1 and Area2 (Fig. 7). To calculate the cumulative correlation values for the parameters Area1 and Area2, their respective areas were

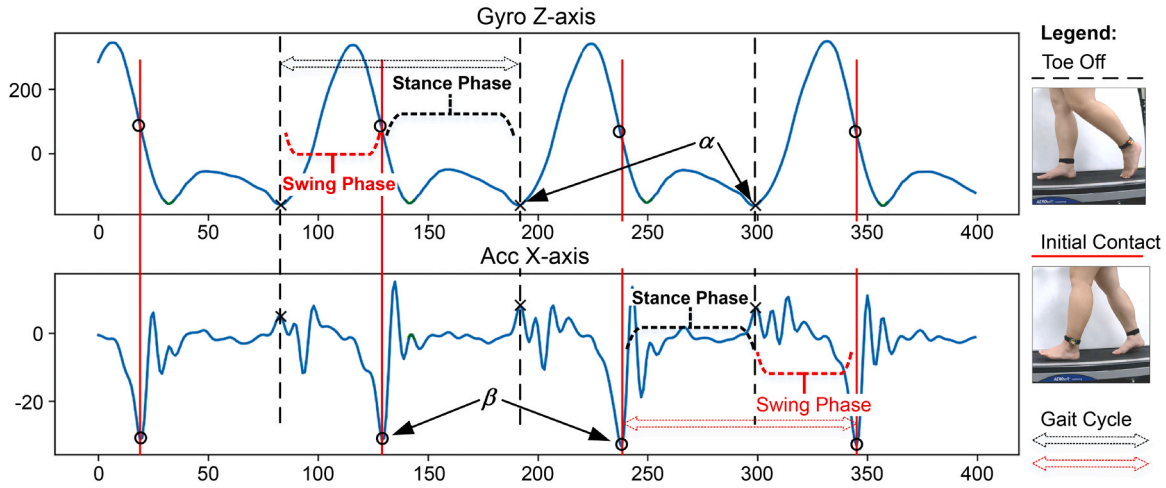

Fig. 5. Signal features on the z-axis of the gyroscopes and the x-axis of the accelerometers to segmentation of the swing phase, stance phase, and gait cycle.

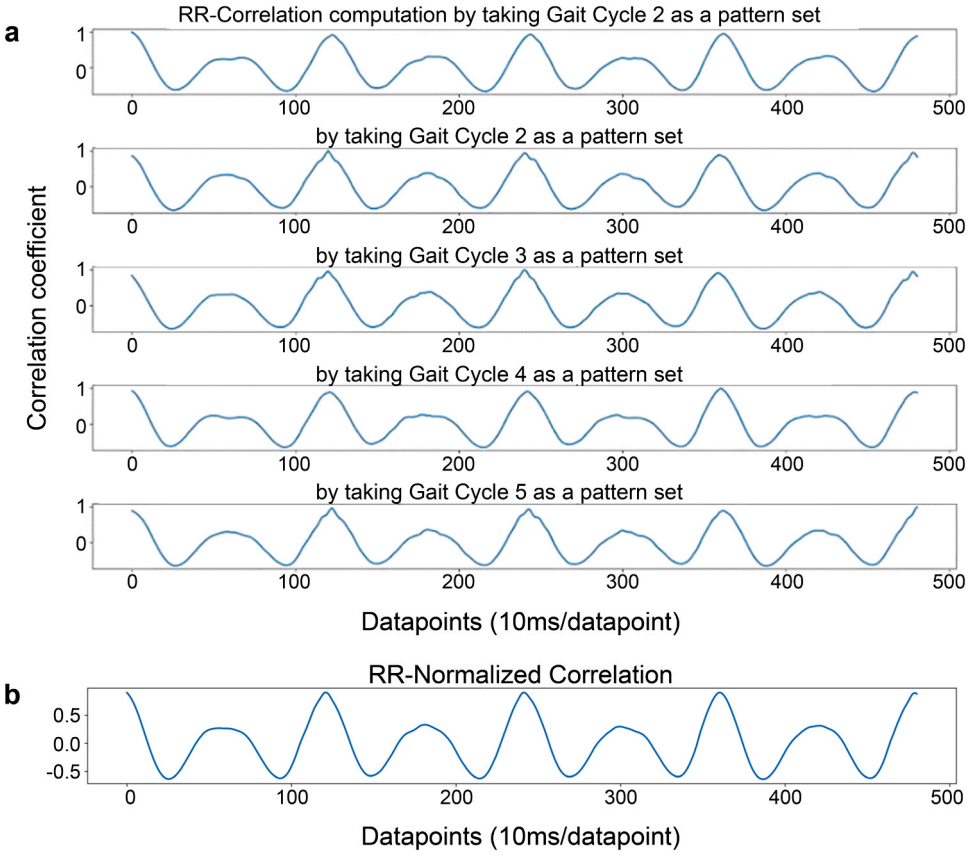

Fig. 6. Autocorrelation/cross-correlation calculation: (a) results of the correlation sequences of the five consecutive gait cycles in a gait record segment; (b) average correlation sequence of the point-to-point averages of the five gait cycles' sequences.

determined by successive summation under the curves.

For all the parameters mentioned above, they are shown in Table 1.

3. Theory

To obtain the most accurate classification of frailty by gait, the selection of an optimal feature set from the features in Table 1 was necessary for intelligent classification. In this study, we adopted a brute-force approach that exhaustively enumerated all subsets of features in Table 1 and tested the effectiveness of each individual subset to be the optimal feature set based on the high computing power of graphics processing units (GPU) systems. Since there are 25 features in Table 1, the total number of subsets that needed to be verified was up to 2^{25} cases. Reducing the number of tested subsets was the major challenge in this situation, even with a GPU system.

To address this challenge, we developed an approach that uses a smaller number of enumerated subsets for incremental improvement. First, we established a set of core features by selecting significant features in Table 1 with statistical analysis. In this way, we only needed to enumerate all subsets without the core features, which can reduce the number of exhaustively enumerated subsets. With incremental improvement, a core feature set is used as a default set, combined with a

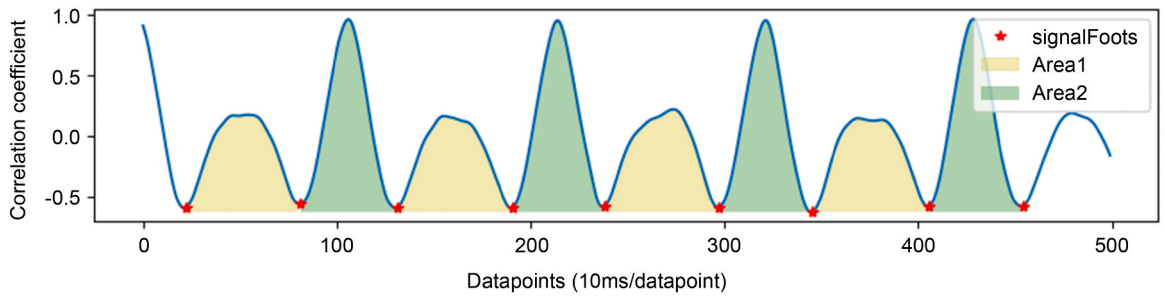

Fig. 7. Structural schematic diagram of the two cumulative correlation parameters, Area1 and Area2, under one autocorrelation/cross-correlation sequence curve.

Table 1
Parameters of the correlation sequence, gait, and cumulative correlation sequence between the non-frail control and frail groups.

Parameter	Control group (n = 22)	Frail group (n = 24)	p-value
Correlation sequence parameters			
RR-μ, mean (SD)	0.0001 (0.007)	0.002 (0.007)	0.48
RR-V, median (IQR)	496.31 (575.66)	327.66 (371.65)	0.65
RR-σ, mean (SD)	0.409 (0.018)	0.412 (0.034)	0.78
LL-μ, mean (SD)	0.002 (0.008)	0.001 (0.009)	0.80
LL-V, median (IQR)	339.81 (721.04)	284.05 (416.20)	0.84
LL-σ, mean (SD)	0.408 (0.019)	0.407 (0.043)	0.89
RL-μ, mean (SD)	−0.0001 (0.008)	0.001 (0.007)	0.53
RL-V, median (IQR)	346.28 (314.97)	314.80 (189.30)	0.70
RL-σ, mean (SD)	0.404 (0.017)	0.404 (0.034)	0.98
LR-μ, median (IQR)	0.003 (0.007)	0.002 (0.005)	0.76
LR-V, median (IQR)	363.86 (427.11)	393.08 (586.57)	0.90
LR-σ, mean (SD)	0.410 (0.018)	0.410 (0.032)	0.97
Gait parameters			
Cadence (step/min), mean (SD)	64.01 (3.21)	72.51 (4.12)	< .001***
GCI (s), mean (SD)	1.12 (0.07)	0.96 (0.07)	< .001***
GCP (s), mean (SD)	4.48 (0.27)	3.85 (0.28)	< .001***
Swing-phase (%), median (IQR)	39.75 (0.98)	38.78 (1.38)	0.005**
Stance-phase (%), median (IQR)	60.25 (0.98)	61.22 (1.38)	0.005**
Cumulative correlation sequence parameters			
RR-Area1, median (IQR)	111.76 (14.69)	111.10 (19.76)	0.90
RR-Area2, median (IQR)	131.98 (13.16)	134.51 (15.66)	0.41
LL-Area1, median (IQR)	109.77 (16.79)	109.10 (19.16)	0.62
LL-Area2, median (IQR)	135.45 (9.72)	137.16 (18.15)	0.62
RL-Area1, mean (SD)	114.50 (12.43)	113.94 (15.50)	0.90
RL-Area2, mean (SD)	136.28 (12.82)	137.63 (12.03)	0.72
LR-Area1, mean (SD)	112.61 (14.09)	113.23 (14.63)	0.89
LR-Area2, median (IQR)	140.87 (14.51)	140.20 (16.38)	0.64

Notes:
1. * indicates a p-value of < 0.05. ** indicates a p-value of < 0.01. *** indicates a p-value of < 0.001.
2. SD, standard deviation. IQR.
3. RR-μ, RR-V, and RR-σ stand for the mean, variation, and standard deviation values of the RR sequence, respectively; the same convention applies for LL, LR, and RL sequences.
4. GCI, single-stride gait cycle interval (Eq. (5)); GCP, 5-stride gait cycle period (Eq. (6)).

subset of the reduced enumeration to verify the effectiveness of the optimality of this combination.

In the last stage, all the features in the created optimal feature set needed to be refined for their contribution to the optimality of the combination. For those features without contribution, they were removed from the optimal feature set.

3.1. Statistical analysis

As outlined by Caby et al. [25], at a 95 % power and a 5 % two-tailed significance level, complete data from at least 24 participants (12 in each experimental group) are required to detect the difference in gait features. We performed a power analysis using G* Power 3.1 software (University of Kiel, Germany) [26]. Descriptive statistics were calculated as the number of units, percent, mean (standard deviation [SD]), and median (interquartile range [IQR]). Continuous variable distributions were evaluated using the Shapiro–Wilk test. To evaluate statistical differences in various parameters, the χ^2 test was used along with Yates correction to compare categorical variables. Conversely, the independent sample t test or Mann–Whitney *U* test was used to compare continuous variables based on the results of normality tests. Statistical significance was set at $p \leq 0.05$.

In particular, the results of the statistical analysis for the proposed parameters in the classification of frailty by gait are shown in Table 1.

3.2. Gait-based frailty classification

In the present study, three supervised machine learning models: the k nearest neighbors (kNN), support vector machine (SVM), and random forest (RF), were used to classify frail gait. kNN [27,28] is a typical machine learning algorithm commonly used for classification and regression tasks. The central idea of kNN is to determine the coordinates in the feature space that are like the target data point. The similarity was measured by calculating the distance between the data points using a mathematically defined or special distance.

SVM [29,30] is a common machine learning algorithm widely used in supervised learning and pattern recognition tasks. It has several advantages, including an ability to extract statistical features from a limited number of training samples, while handling high-dimensional data and non-linear problems. SVM is used to find the optimal hyperplane in the feature space to separate different classes of data. These boundaries, along with the hyperplanes, form the classification decision boundary, which is used to distinguish data from different data categories.

RF is an ensemble learning algorithm that comprises multiple decision trees. It improves the accuracy of the model by combining the prediction results of these decision trees. In the RF algorithm, the training process includes two primary methods for introducing randomness: bootstrap aggregation (or bagging) and feature random selection. The introduction of randomness not only increases the diversity of the model but also prevents it from overfitting.

3.3. Optimal feature set extraction

Through statistical analysis, the present study used the proposed parameters with statistical significance ($p \leq 0.05$) as an initial core feature set, named SA, to recognize frailty states by gait. To explore the optimal feature set for the three classification algorithms, we proposed an optimal feature set extraction (OFSE) scheme. This scheme comprises three stages: initial, enumeration, and refinement. In the initial phase, the SA set is generated to reduce the number of enumerations of all possible feature combinations, thus increasing efficiency in creating optimal feature sets for the frailty classification. Subsequently, all

possible combinations of features are enumerated exhaustively, and each combination is tested to create the optimal set of features. Finally, to prove that each element feature in the optimal set is necessary for the frailty classification, the optimal set is tested again for optimality by excluding one element feature at a time.

3.3.1. OFSE algorithm

Initial stage: Using statistical analysis, select parameters (see Table 1) with a condition of $p \leq 0.05$ (using independent sample *t* tests or Mann–Whitney *U* tests) are used to form a preliminary set of initial core features, i.e., the SA set.

Enumeration stage: Let SPP be the set of proposed parameters (Table 1). Enumerate exhaustively all the remaining parameters beyond SA (that is, the parameters with $p > 0.05$) to form the set (SPP−SA) and its power set, named $\mathcal{P}$(SPP−SA), which constitutes all subsets of (SPP−SA).

1. Select an element set ES from $\mathcal{P}$(SPP−SA) that has not been previously evaluated and subsequently create a union with SA. Evaluate the identification performance of the union set (that is, (SA∪ES)) using a selected classification algorithm (kNN, SVM, or RF).
2. If the recognition performance of the current case, (SA∪ES), is better than the old recorded best union set Best_Set, then update the old record, i.e., Best_Set = (SA∪ES).
3. Check whether all the elements in $\mathcal{P}$(SPP−SA) have been evaluated; if so, exit this stage; otherwise, go to Step 1.

   Refinement stage: Refine the best union set, *i.e.* Best_Set, obtained in the last stage.
4. Remove an element parameter *p* from the Best_Set that has not been previously evaluated and then evaluate the classification performance of the new set (Best_Set−{*p*}), using the selected classification algorithm.
5. If the classification performance of the set is equal to or better than that of Best_Set, set Best_Set = (Best_Set−{*p*}).
6. Check whether all elements in the Best_Set have been evaluated; if so, exit this stage; otherwise, go to Step 4.

4. Results

To obtain reliable prediction results for the classifications in this study, we adopted a five-fold stratified cross-validation, a commonly used evaluation technique for classification models in machine learning. This method divides the training data set into five subsets, where each subset is composed of the elements equally from the frailty and non-frail control groups, to evaluate the classification performance. Each subset served as an independent validation set, while the remaining subsets were used for model training. This approach can process many experimental data while reducing the risks of overfit during the training process. The expressions of the classifier performance evaluation metrics, such as accuracy, sensitivity, specificity, precision, and F1-score, are as follows (Eqs. (7–11)) (true positive, TP; false positive, FP; false negative, FN; true negative, TN).

$$Accuracy = \frac{TP + TN}{TP + FP + FN + TN} \tag{7}$$

$$Sensitivity = \frac{TP}{TP + FN} \tag{8}$$

$$Specificity = \frac{TN}{TN + FP} \tag{9}$$

$$Precision = \frac{TP}{TP + FP} \tag{10}$$

$$F1 - score = \frac{2 \times (Sensitivity \times Precision)}{Sensitivity + Precision} \tag{11}$$

This study enrolled 46 participants, including 24 frail participants (9 men; mean age [SD]: 74.8 [3.9] years) and 22 non-frail controls (3 men, p-value = 0.16; mean age [SD]: 74.2 [4.7] years, p-value = 0.66) (Appendix A). In Table 1, it shows the gait features of participants in the frail and non-frail control groups.

4.1. Evaluation of feature sets

Table 1 presents the p-values of all proposed gait features obtained by statistical analysis, which could be used to select qualified gait features for the best set of features. Although the SA set (see Table 2) could be applied to kNN, SVM, and RF algorithms, other optimal feature sets for different classification algorithms may exist to identify the frailty state of older adults. As such, the OFSE scheme described above could be applied to produce a separate optimal feature set for each classification algorithm. Table 2 presents the optimal feature sets corresponding to the statistical analysis and each classification algorithm derived in this study.

Before intelligent recognition with the optimal feature sets is performed, each algorithm needs to adjust the hyperparameters to obtain the best classification results. For kNN, for each new set of features, the k-value of the nearest neighbors is tested from 1 to 10, where the k-value with the best results is chosen. When designing an SVM model, the selection of hyperparameters that include cost and gamma parameters is crucial. When selecting parameters for our SVM model, a grid search method was used. This can help to identify the best combination and maximize model performance and generalizability by systematic search and evaluation within the predefined parameter range. To verify the reliability of grid search results, SVM models use various kernel functions (such as linear functions, polynomial functions, and radial basis functions), which can reduce the computational complexity of machine learning and avoid dimensional problems. In the RF model, the hyperparameters include the number of decision trees and the features that each tree considers when splitting nodes. For hyperparameter tuning, we repeatedly applied the entire five-fold cross-validation process, each time using different model settings. We subsequently compared all the models, choose the best, train them in a complete training set, and then evaluate them in a test set.

Table 2 presents four tested sets for the best feature extraction, SA, kNN_best, SVM_best, and RF_best. To evaluate the four tested sets by the chosen recognition algorithms, the combinations include SA with kNN, SVM, and RF, respectively, as well as kNN with kNN_best, SVM with SVM_best, RF with RF_best, *etc.* Consequently, the combinations tested with the confusion matrices are summarized in Table 3. In this table, we find that the performance metrics (Eqs. (7–11)) with the statistical extraction of gait features achieved good results when classifying frailty states. All performance figures exceeded 84 %. However, the OFSE scheme could generate the truly optimal feature set of the separate recognition algorithm, as presented in Table 3. Similarly, the

Table 2
The optimal feature sets derived from the statistical approach and OFSE with the kNN, SVM, and RF classification algorithms.

Approach	Derived optimal feature set
Statistical approach	SA = {Cadence, GCI, GCP, Swing phase, Stance phase}
OFSE with kNN	kNN_best = {Cadence, GCI, GCP, Swing phase, Stance phase, RR-μ, RR-σ, LL-μ, LL-σ}
OFSE with SVM	SVM_best = {GCP, Swing phase, Stance phase, RR-μ, RL-μ, RL-V, RL-σ}
OFSE with RF	RF_best = {Cadence, GCI, GCP, LL-σ, RL-μ, LR-σ}

Notes:
1. GCI, single-stride gait cycle interval (Eq. (5)); GCP, 5-stride gait cycle period (Eq. (6)).
2. kNN: k-nearest neighbor; SVM: support vector machine; RF: random forest; OFSE: optimal feature set extraction.

Table 3
The predictive results of the gait-based frailty status in combinations of various feature selection methods and classification algorithms.

Feature selections				kNN		SVM		RF	
Statistical extraction	Truth label		**F**	22	2	21	3	20	4
(with the SA set for all classification algorithms)	**(Confusion Matrix)**		**NF**	3	19	3	19	3	19
				F	**NF**	**F**	**NF**	**F**	**NF**
				Predicted label					
	Accuracy (%)			89.1		86.9		84.7	
	Precision (%)			89.2		86.3		82.6	
	Sensitivity (%)			89		86.3		86.3	
	Specificity (%)			89.2		87.5		83.3	
	F1 Score (%)			89		86.3		84.4	
Optimal feature set extraction	Truth label	**F**		23	1	23	1	23	1
(with kNN_best for kNN, SVM_best for SVM, and RF_best for RF)	**(Confusion Matrix)**	**NF**		2	20	1	21	1	21
				F	**NF**	**F**	**NF**	**F**	**NF**
				Predicted label					
	Accuracy (%)			93.9		95.7		95.7	
	Precision (%)			95.2		95.6		95.6	
	Sensitivity (%)			90.9		95.6		95.6	
	Specificity (%)			95.8		95.8		95.8	
	F1 Score (%)			93.3		95.6		95.6	

Notes:
1. F: frail group; NF: non-frail control group.
2. kNN: k-nearest neighbor; SVM: support vector machine; RF: random forest.

performance metrics produced by the OFSE scheme are higher than the statistical extraction about 4–11 %.

In the present study, the completion of the production of the optimal feature sets with corresponding recognition algorithms consumes significant computing power due to the exhaustive enumeration strategy used in feature set extraction. The computer system used for signal processing and data analysis in this study is equipped with a GPU device, as presented in Table 4. The time spent generating kNN_best, SVM_best, and RF_best is also shown. In fact, the results of the frailty classification in Table 4 are based on the optimal feature sets that took 3.26 days to fully calculate.

4.2. Gait-based frailty status classification

The five aspects used to evaluate the classification of the frailty status according to gait are presented in Table 3. For the statistical extraction, the SA set generated by statistical analysis is applied as a feature set with kNN, SVM, and RF, respectively. The classification results showed that kNN has the highest performance metrics over 89 %. Subsequently, the SVM performance metrics fell short of kNN but remained above 86 %. Although the result of the RF classification is not as good as the previous two, it remained above 84 % on average.

For the optimal feature set extraction, the SVM with SVM_best and the RF with RF_best perform the best, achieving the same performance metrics. The kNN with kNN_best falls short of the other classification algorithms due to its lower sensitivity (90.9 %). However, all classification algorithms that used the OFSE algorithm produced better performance than statistical extraction (Table 3).

Table 4
The computer equipment and time spent on computation.

Computer components		Software platform	
CPU: Intel Core i5–10400		OS: Windows 10 22H2	
GPU: NVIDIA GeForce RTX2080 8 GB		Programming language: Python 3.7.9	
RAM: 40 GB			
Storage: 1 TB			
	kNN_best	**SVM_best**	**RF_best**
Time used	1654 min 4.6 s (≈ 1.15 days)†	1465 min 2.3 s (≈ 1.02 days)†	1576 min 56.4 s (≈ 1.09 days)†

Note: † indicates the nearest equivalent time period in days.
GPU: graphics processing units; OS: operating system; kNN: k-nearest neighbor; SVM: support vector machine; RF: random forest.

From among the observations presented in Table 2, a few points are interesting in relation to the contribution of the gait features proposed in this investigation to the classification of frailty. The points are related to what the truly core features are and their performance behavior. Some of the features in Table 2 are partially common (such as Cadence, GCI, Swing-Phase, Stance-Phase, *etc.*) among the four sets, while others are common, such as GCP. To explore these interesting points, we created the intersection and union of the four sets (*i.e.*, SA, kNN_best, SVM_best, and RF_best in Table 2) below.

Feature_Set_Intersection (FSI) = {GCP}.

Feature_Set_Union (FSU) = {Cadence, GCI, GCP, Swing-Phase, Stance-Phase, RR-μ, RR-σ, LL-μ, LL-σ, RL-μ, RL-V, RL-σ, LR-σ}.

The performance comparison between the feature sets produced by different approaches, such as SA by the statistical extraction, the sets by the optimal feature set extraction, FSI, and FSU are presented in Table 5. The performance metrics from the statistical extraction were obtained by the corresponding performance metrics while applying the kNN, SVM, and RF algorithms with SA. For the performance metrics derived from the optimal feature set extraction, FSI, and FSU, their situations are the same as those of the statistical extraction.

From the observations presented in Table 5, we were able to identify that the feature set of the frailty classification with gait produced by statistical analysis is good enough in all performance metrics (> 84 %). The OFSE scheme contributes optimal performance metrics (all > 93 %) to the gait frailty classification. In addition, we found that the FSI set with a single element GCP could achieve performance metrics of > 80 %

Table 5
Performance metrics of the various feature sets and their extraction strategies assessed using the k-nearest neighbor, support vector machine, and random forest models.

Performance metrics	**Core feature by statistical analysis**	**Optimal feature by the OFSE scheme**	**Intersection of the four feature sets (FSI)**	**Union of the four feature sets (FSU)**
Accuracy (%)	86.2	95.1	81.1	67.4
Precision (%)	85.1	95.5	81.2	62.3
Sensitivity (%)	86.3	94	78.8	57.5
Specificity (%)	86.1	95.8	83.3	76.4
F1 Score (%)	85.7	94.8	79.9	59.1

OFSE: optimal feature set extraction.

in the gait frailty classification, which was superior to the FSU set involved in the gait frailty classification by approximately 14 %. Therefore, the addition of more features involved in the classification of gait frailty may not yield good results.

5. Discussion

This study used wireless IMUs to collect and analyze gait signals from non-frail and frail older adults, with the aim of developing a gait-based frailty detection method. Given the limited scientific evidence supporting gait as a frailty indicator, more research is needed to address this gap. In addition to conventional gait parameters (e.g., Cadence, GCI) obtained from gait experiments, we introduced novel parameters (e.g., RR-μ, RR-Area1) derived from autocorrelation and cross-correlation analyses (Table 1). Although these correlation-based parameters did not show statistical significance (all $p > 0.05$, Table 1), their application in frailty classification (Table 2) significantly improved performance, as demonstrated in Table 3. For example, when only conventional parameters were used (the SA set, Table 2), the classification accuracy remained below 90 % (Table 3). On the contrary, incorporating correlation-derived parameters (e.g., RR-μ, RL-μ) in the same classifications, such as kNN_best, SVM_best, and RF_best (Table 2), improved performance to more than 90 % (Table 3), underscoring their utility in frailty assessment.

The exhaustive enumeration strategy of the OFSE scheme for feature selection would require calculating 2^{25} cases to determine the optimal feature sets for different recognition algorithms, resulting in impractical computational time. To address this, we adopted the SA set created by statistical analysis as the initial core feature set, significantly reducing the number of cases from 2^{25} to 2^{20}. Using a GPU system, the total computation time to identify all optimal feature sets was approximately 3.26 days (see Table 4), achieving a 97 % reduction in processing time compared to the original approach.

As demonstrated in Table 5, the proposed OFSE scheme achieved superior performance in gait-based frailty classification compared to alternative methods, achieving approximately 95 % accuracy. This high classification performance confirms the clinical utility of gait features for assessing frailty in older adults. In particular, the GCP gait parameter emerged as particularly significant for frailty detection, as it alone achieved 80 % classification accuracy. This finding aligns with previous research linking frailty to fall risk and fear of falling [31], which often manifests itself as cautious gait patterns characterized by reduced speed and shorter stride length [32,33]. Such gait modifications may explain the observed reduction in GCP among frail older adults compared to their non-frail counterparts.

In recent studies, Zanotto et al. found that traditional mobility parameters yielded accuracy rates of 73–87 % for frailty in an older population [34]. Lien et al. analyzed gait signals acquired from tri-axial accelerometry and reported that kNN F1 scores with x-axis components of 92 % for non-fallers and 89 % for recurrent fallers; additionally, the RSS values of the signals were 95 % for non-fallers and 94 % for recurrent fallers [24]. The kNN classification of gait stability and symmetry accurately distinguished non-fallers from recurrent fallers. Specifically, RSS-based cross-correlation coefficients could serve as effective gait features to assess the risk of falls in older adults [24].

Compared with previous research, our investigation has two advantages. First, we adopted wireless IMUs to collect and analyze gait signals from both non-frail and frail older individuals to detect frailty; wireless IMUs are also convenient and have a lower detection cost when utilized for health management and fall injury prevention for community-dwelling older adults. Second, our approach adopted supervised machine learning methods, such as kNN, SVM, and RF models, applied for classification, achieving accuracies of 94 %, 96 %, and 96 %, respectively. These accuracies indicate the value of early and accurate identification of frailty, which allows for timely interventions to prevent falls [35], functional decline, and hospitalization while supporting personalized care planning. Our system provides a scalable and objective tool for researchers and clinicians to monitor frailty in community settings, improving preventive healthcare and contributing to aging-in-place strategies. Therefore, we confirm that the use of gait signals to identify frail older individuals is feasible with very high accuracy.

Although our model achieved high sensitivity (95.6 %) and specificity (95.8 %) in frailty classification (Table 3), we recognize the clinical importance of considering misclassification outcomes. In the event of false positives (around 4.2 % of cases), it can lead to unnecessary interventions, including additional clinical evaluations or preventive measures, potentially increasing healthcare costs and patient anxiety. However, in frailty screening, such over-detection is generally preferable to under-detection, as it allows for early monitoring of at-risk individuals. The occurrence of false negatives (around 4.4 % of cases) poses a greater concern, as delayed identification of frailty could postpone critical interventions (e.g., strength training, nutritional support), accelerating functional decline. This risk underscores the need for periodic reassessment in clinical practice, even when initial screenings are negative.

The balanced performance of our model (demonstrating approximately 95 % accuracy for both classes) suggests its clinical implementation would yield substantially more benefits than risks. This performance advantage is particularly notable when compared with conventional screening tools like the Fried criteria, which typically exhibit 10–15 % error rates in community settings [32]. Our approach holds important clinical implications for monitoring and managing frail older adults. Through non-invasive gait signal acquisition, we can continuously track participants' gait deterioration, enabling (1) early detection of declining mobility patterns, (2) fall risk prevention [33], and (3) AI-assisted personalized care plans for community-dwelling older adults. These capabilities facilitate timely intervention and support the development of tele-rehabilitation systems for frail populations.

5.1. Strengths and limitations

While several recent studies have explored the use of inertial sensor-based gait analysis for frailty prediction, stratification, or fall risk assessment [36–41], our study makes a distinct contribution by proposing an optimal feature set extraction scheme combined with supervised machine learning algorithms, achieving a classification accuracy up to 96 %. For example, Toda and Chin predicted physical frailty using cane usage characteristics during walking, focusing only on cane users with lower model accuracy [36]. Amjad et al. analyzed the evolution of frailty assessment with IMU-based gait data and machine learning, noting the strong performance of kNN, SVM, and RF, but without emphasis on model optimization [37]. Neira Álvarez et al. stratified older adults by frailty and falls using gait parameters but did not perform direct frailty classification [38], while Pierleoni et al. developed an optimized mobility evaluation system with lower accuracy than ours [39]. Fan et al. combined wearable gait sensors with machine learning but placed less emphasis on signal processing [40], and Ruiz-Ruiz et al. presented a review of significant gait parameters without proposing a classification model [41]. In contrast, our work integrates core gait metrics with correlation-based features and leverages GPU-accelerated computation to optimize model performance, thereby advancing the precision of frailty classification. The SVM and RF models achieved an excellent accuracy of 96 %, whereas the kNN model reached an accuracy of 94 %. Nevertheless, this study had some limitations that should be acknowledged. First, this study employed a cross-sectional design, meaning that data were collected at a single point in time rather than over a period. As a result, we could not establish any causal relationship between gait changes and frailty. Thus, future longitudinal studies are required to develop a classification algorithm for gait assessment related to frailty, which would improve our understanding of how gait changes relate to frailty. Furthermore, the wearable sensors used in this study

lacked magnetometers for directional measurement and surface electromyography to measure muscle activation. As such, new studies using wearable sensors along with accelerometers, gyroscopes, and other enhancements are required to maximize wireless IMU functions.

5.2. Novelty and possible health implications of the findings

In the present study, we combined the gait correlational parameters with kNN, SVM, and RF to obtain robust classification results that helped distinguish non-frail older adults from frail older adults. Our results, combined with those of recent studies, strengthen the role of gait correlational parameters in the detection of frailty in older adults. Instrumental gait analysis combined with kNN, SVM, and RF algorithms may be used to identify frail older adults for improved management and reduced healthcare burdens primarily in community-dwelling older adults.

5.3. Future directions

In future studies, greater diversity in participant characteristics, such as sex, age groups, and functional status, should be considered to improve the generalizability and applicability of the classification models across broader older adult populations. Future studies should also include larger numbers of frail patients with different CHS scores to expand the clinical impact of these algorithms. Moreover, longitudinal studies should be conducted to explore the gait changes that occur after frailty diagnosis.

6. Conclusion

Overall, this study demonstrated the potential of using wireless IMUs to collect and analyze gait signals to identify frail older individuals. Our findings highlight the effectiveness of supervised machine learning models, such as kNN, SVM, and RF, in classifying frailty-related gait patterns among older adults. As such, the present study provides a crucial reference for the future development of intelligent and age-friendly telehealth monitoring systems to protect older adults against the health consequences of frailty especially when considering climate change.

The SA set showed sufficient performance in all performance metrics in the SVM, kNN, and RF classifiers (> 84 %). The OFSE scheme, which enumerates exhaustively all remaining parameters beyond SA, contributes the optimal performance metrics (almost all > 95 %) to the gait frailty classification. Furthermore, we found that the feature set intersection with a period of multiple gait cycles could achieve performance metrics of almost > 80 % in the gait frailty classification.

Our findings further suggest that using gait features based on wireless IMUs can help to improve the objectivity and accuracy of frailty status classification; using the OFSE scheme to enumerate all remaining parameters beyond SA further optimizes performance metrics and can be used to adjust telehealth care plans.

CRediT authorship contribution statement

Bo Liu: Writing – review & editing, Visualization, Investigation, Formal analysis, Data curation, Conceptualization. **Chien-Hsiang Chang:** Writing – original draft, Visualization, Software, Investigation, Formal analysis, Data curation, Conceptualization. **Wen-Fong Wang:** Writing – review & editing, Writing – original draft, Visualization, Validation, Supervision, Software, Resources, Project administration, Methodology, Investigation, Funding acquisition, Formal analysis, Data curation, Conceptualization. **Danyal Shahmirzadi:** Writing – original draft, Visualization, Validation, Software, Methodology, Formal analysis, Data curation, Conceptualization. **Wei Huang:** Writing – original draft, Visualization, Investigation, Formal analysis, Data curation, Conceptualization. **Wei-Chih Lien:** Writing – review & editing, Writing – original draft, Visualization, Validation, Resources, Project administration, Methodology, Investigation, Funding acquisition, Formal analysis, Data curation, Conceptualization. **Yang-Cheng Lin:** Writing – review & editing, Writing – original draft, Visualization, Validation, Supervision, Software, Resources, Project administration, Methodology, Investigation, Funding acquisition, Formal analysis, Data curation, Conceptualization. **Tai-Hua Yang:** Writing – original draft, Validation, Resources, Methodology, Conceptualization. **Yi-Ching Yang:** Writing – original draft, Validation, Resources, Methodology, Conceptualization. **Wei-Ming Wang:** Writing – original draft, Validation, Methodology, Conceptualization. **Ta-Shen Kuan:** Writing – original draft, Validation, Resources, Methodology, Conceptualization.

Ethical considerations

This study was approved by the Institutional Review Board of National Cheng Kung University (no. NCKU HREC-F-109–497–2). All the participants provided written or oral informed consent.

Funding

This work was supported by the National Cheng Kung University Hospital [grant number NCKUH-11102063]; National Cheng Kung University, within the framework of the Higher Education Sprout Project by the Ministry of Education (MOE) in Taiwan [grant number D112-F2335]; the MOE Teaching Practice Research Program title with Post-Pandemic Curriculum-Redesign for Flipped Learning in Rehabilitation Medicine: Introducing “AI-based functional mobility assessment” technology into the training curriculum to improve the mobility assessment skills of medical students [grant number PMN1120522]; the National Science and Technology Council [grant number NSTC 111-2314-B-006-064-MY3 for a 3-year project, NSTC 113-2637-E-224-002-, and NSTC 114-2425-H-006-007-]; and the "Intelligent Recognition Industry Service Center" from the Featured Areas Research Center Program within the framework of the Higher Education Sprout Project (Yuntech ID: 113-N04-2) by the MOE in Taiwan. The financial sponsors played no role in the study design and execution, the analysis and interpretation of data, or in writing the manuscript. None of the statements in this manuscript, including the results and conclusions, necessarily represents the official views of the funding agencies.

Declaration of Competing Interest

The authors declare that they have no known competing financial interests or personal relationships that could have appeared to influence the work reported in this paper.

Acknowledgments

The authors would like to thank Yu-Yi Pan, Department of Statistics, College of Management, National Cheng Kung University for providing statistical consulting services. In addition, we would also like to thank Yu-Ching Hung of the Department of Computer Science and Information Engineering, National Yunlin University of Science and Technology, for her assistance in processing the performance metrics of the experimental data.

Appendix A. Supporting information

Supplementary data associated with this article can be found in the online version at doi:10.1016/j.csbj.2025.05.011.

Data availability

The original contributions presented in the study are included in the article/Supplementary Material. Further inquiries can be directed to the

corresponding authors.

References

[1] Ofori-Asenso R, Chin KL, Mazidi M, Zomer E, Ilomaki J, et al. Global incidence of frailty and prefrailty among community-dwelling older adults: a systematic review and meta-analysis. JAMA Netw Open 2019;2:e198398.

[2] Petermann-Rocha F, Pell JP, Celis-Morales C, Ho FK. Frailty, sarcopenia, cachexia and malnutrition as comorbid conditions and their associations with mortality: a prospective study from UK Biobank. J Public Health (Oxf) 2022;44:e172–80.

[3] Doody P, Lord JM, Greig CA, Whittaker AC. Frailty: pathophysiology, theoretical and operational definition(s), impact, prevalence, management and prevention, in an increasingly economically developed and ageing world. Gerontology 2023;69:927–45.

[4] To TL, Doan TN, Ho WC, Liao WC. Prevalence of frailty among community-dwelling older adults in asian countries: a systematic review and meta-analysis. Healthc (Basel) 2022;10:895.

[5] Hommen JM, Batista JP, Bollheimer LC, Hildebrand F, Laurentius T, et al. Movement patterns during gait initiation in older adults with various stages of frailty: a biomechanical analysis. Eur Rev Aging Phys Act 2024;21(1).

[6] Martinikorena I, Martínez-Ramírez A, Gómez M, Lecumberri P, Casas-Herrero A, et al. Gait variability related to muscle quality and muscle power output in frail nonagenarian older adults. J Am Med Dir Assoc 2016;17:162–7.

[7] Valdés-Aragonés M, Pérez-Rodríguez R, Carnicero JA, Moreno-Sánchez PA, Oviedo-Briones M, et al. Effects of monitoring frailty through a mobile/web-based application and a sensor kit to prevent functional decline in frail and prefrail older adults: FACET (Frailty Care and Well Function) pilot randomized controlled trial. J Med Internet Res 2024;26:e58312.

[8] Vollenbroek-Hutten M, Jansen-Kosterink S, Tabak M, Feletti LC, Zia G, et al. Possibilities of ICT-supported services in the clinical management of older adults. Aging Clin Exp Res 2017;29:49–57.

[9] Keränen NS, Kangas M, Immonen M, Similä H, Enwald H, et al. Use of information and communication technologies among older people with and without frailty: a population-based survey. J Med Internet Res 2017;19:e29.

[10] Dent E, Hanlon P, Sim M, Jylhävä J, Liu Z, et al. Recent developments in frailty identification, management, risk factors and prevention: a narrative review of leading journals in geriatrics and gerontology. Ageing Res Rev 2023;91:102082.

[11] Minici D, Cola G, Giordano A, Antoci S, Girardi E, et al. Towards automated assessment of frailty status using a wrist-worn device. IEEE J Biomed Health Inf 2022;26:1013–22. https://doi.org/10.1109/JBHI.2021.3100979.

[12] Camerlingo N, Shaafi Kabiri N, Psaltos DJ, Kelly M, Wicker MK, et al. Monitoring gait and physical activity of elderly frail individuals in free-living environment: a feasibility study. Gerontology 2024;70:439–54. https://doi.org/10.1159/000535283.

[13] Seel T, Raisch J, Schauer T. IMU-based joint angle measurement for gait analysis. Sensors 2014;14:6891–909.

[14] Demarteau J, Jansen B, Van Keymolen B, Mets T, Bautmans I. Trunk inclination and hip extension mobility, but not thoracic kyphosis angle, are related to 3D-accelerometry based gait alterations and increased fall-risk in older persons. Gait Posture 2019;72:89–95.

[15] Suri A, VanSwearingen J, Rosano C, Brach JS, Redfern MS, et al. Uneven surface and cognitive dual-task independently affect gait quality in older adults. Gait Posture 2023;106:34–41.

[16] Bortone I, Sardone R, Lampignano L, Castellana F, Zupo R, et al. How gait influences frailty models and health-related outcomes in clinical-based and population-based studies: a systematic review. J Cachex– Sarcopenia Muscle 2021;12:274–97.

[17] Sun CY, Hsu LC, Su CC, Li CY, Chao CT, et al. Gait abnormalities and longitudinal fall risk in older patients with end-stage kidney disease and sarcopenia. BMC Geriatr 2024;24:937.

[18] Wang JJ. Psychological abuse and its characteristic correlates among elderly Taiwanese. Arch Gerontol Geriatr 2006;42:307–18. https://doi.org/10.1016/j.archger.2005.08.006.

[19] Fried LP, Tangen CM, Walston J, Newman AB, Hirsch C, et al. Frailty in older adults: evidence for a phenotype. J Gerontol A Biol Sci Med Sci 2001;56:M146–57.

[20] Schafer RW. What is a Savitzky-Golay filter? [lecture notes]. IEEE Signal Process Mag 2011;28:111–7.

[21] Mello RGT, Oliveira LF, Nadal J. Digital Butterworth filter for subtracting noise from low magnitude surface electromyogram. Comput Methods Prog Biomed 2007;87:28–35.

[22] Choudhury D. In education and training in optics and photonics. Proc SPIE 2020;104520Y.

[23] Nelson-Wong E, Howarth S, Winter DA, Callaghan JP. Application of autocorrelation and cross-correlation analyses in human movement and rehabilitation research. J Orthop Sports Phys Ther 2009;39:287–95.

[24] Lien WC, Ching CT, Lai ZW, Wang HD, Lin JS, et al. Intelligent fall-risk assessment based on gait stability and symmetry among older adults using tri-axial accelerometry. Front Bioeng Biotechnol 2022;10:887269.

[25] Caby B, Kieffer S, de Saint Hubert M, Cremer G, Macq B. Feature extraction and selection for objective gait analysis and fall risk assessment by accelerometry. Biomed Eng Online 2011;10(1).

[26] Faul F, Erdfelder E, Lang AG, Buchner A. G*Power 3: a flexible statistical power analysis program for the social, behavioral, and biomedical sciences. Behav Res Methods 2007;39:175–91.

[27] Cover T, Hart P. Nearest neighbor pattern classification. IEEE Trans Inf Theory 1967;13:21–7.

[28] Zhang Z. Introduction to machine learning: k-nearest neighbors. Ann Transl Med 2016;4:218.

[29] Awad M, Khanna R. Support vector machines for classification. Effic Learn Mach 2015:39–66.

[30] Sheykhmousa M, Mahdianpari M, Ghanbari H, Mohammadimanesh F, Ghamisi P, et al. Support vector machine versus random forest for remote sensing image classification: a meta-analysis and systematic review. IEEE J Sel Top Appl Earth Obs Remote Sens 2020;13:6308–25.

[31] de Souza LF, Canever JB, Moreira BS, Danielewicz AL, de Avelar NCP. Association between fear of falling and frailty in community-dwelling older adults: a systematic review. Clin Inter Aging 2022;17:129–40.

[32] Hulleck AA, Menoth Mohan D, Abdallah N, El Rich M, Khalaf K. Present and future of gait assessment in clinical practice: towards the application of novel trends and technologies. Front Med Technol 2022;4:901331.

[33] Suri A, Hubbard ZL, VanSwearingen J, Torres-Oviedo G, Brach JS, et al. Fear of falling in community-dwelling older adults: what their gait acceleration pattern reveals. Comput Methods Prog Biomed 2024;244:108001.

[34] Zanotto T, Mercer TH, van der Linden ML, Koufaki P. Screening tools to expedite assessment of frailty in people receiving haemodialysis: a diagnostic accuracy study. BMC Geriatr 2021;21:411.

[35] Leoste J, Strömberg-Järvis K, Robal T, Marmor K, Kangur K, et al. Testing scenarios for using telepresence robots in healthcare settings. Comput Struct Biotechnol J 2024;24:105–14.

[36] Toda H, Chin T. Physical frailty prediction using cane usage characteristics during walking. Sensors 2024;24:6910. https://doi.org/10.3390/s24216910.

[37] Amjad A, Qaiser S, Błaszczyszyn M, Szczęsna A. The evolution of frailty assessment using inertial measurement sensor-based gait parameter measurements: a detailed analysis. Wiley Interdiscip Rev: Data Min Knowl Discov 2024;14:e1557.

[38] Neira Álvarez M, Huertas-Hoyas E, Novak R, Sipols AE, García-Villamil-Neira G, et al. Stratification of older adults according to frailty status and falls using gait parameters explored using an inertial system. Appl Sci 2024;14:6704. https://doi.org/10.3390/app14156704.

[39] Pierleoni P, Belli A, Pinti F, Paoletti M, Raggiunto S, et al. An optimized system for mobility evaluation in frailty phenotype assessment. J Ambient Intell Hum Comput 2024;15:2691–8. https://doi.org/10.1007/s12652-022-03802-3.

[40] Fan S, Ye J, Xu Q, Peng R, Hu B, et al. Digital health technology combining wearable gait sensors and machine learning improve the accuracy in prediction of frailty. Front Public Health 2023;11:1169083. https://doi.org/10.3389/fpubh.2023.1169083.

[41] Ruiz-Ruiz L, Jimenez AR, Garcia-Villamil G, Seco F. Detecting fall risk and frailty in elders with inertial motion sensors: a survey of significant gait parameters. Sensors 2021;21:6918. https://doi.org/10.3390/s21206918.